LA-UR-79-2846

TITLE: R-MATRIX ANALYSES OF LIGHT-ELEMENT REACTIONS FOR FUSION APPLICATIONS

AUTHOR(S): [illegible] N. Hale and P. G. Young

SUBMITTED TO: To be presented at the International Conference on Nuclear Cross Sections for Technology, Knoxville, TN Oct. 22-26, 1979

MASTER

By acceptance of this article for publication, the publisher recognizes the Government's license rights in any copyright and the Government and its authorized representatives have unrestricted right to reproduce in whole or in part said article under any copyright secured by the publisher.

The Los Alamos Scientific Laboratory requests that the publisher identify this article as work performed under the auspices of the USERDA

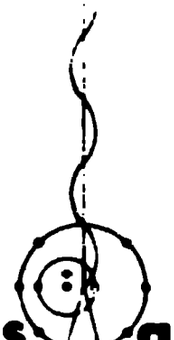

los alamos
scientific laboratory
of the University of California
LOS ALAMOS, NEW MEXICO 87545

An Affirmative Action/Equal Opportunity Employer

UNITED STATES
ENERGY RESEARCH AND
DEVELOPMENT ADMINISTRATION
CONTRACT W-7405-ENG. 36

R-MATRIX ANALYSES OF LIGHT-ELEMENT REACTIONS FOR FUSION APPLICATIONS

G. M. Hale and D. C. Dodder
Los Alamos Scientific Laboratory, University of California
Theoretical Division
Los Alamos, New Mexico 87545, USA

[illegible] reactions, multichannel R-matrix analyses, evaluated fusion cross sections, [illegible]

[illegible] R-matrix analyses of reactions in light systems done at LASL [illegible] of interest in fusion applications. Results of analyses of [illegible] nucleon systems are presented, with particular [illegible] and [illegible] fusion reactions.

Introduction

[illegible] energy from the [illegible] stage, the need for [illegible] reactions [illegible] Many [illegible] charged particles [illegible] energy [illegible] of the reaction, [illegible] to heat the plasma, in removing and replacing the primary fuels, and in providing diagnostic information about plasma conditions.

[illegible] at energies [illegible]

[illegible]

[illegible] R-matrix theory for describing [illegible] has been pointed out at several previous technical conferences.[-7] In the case of charged-particle reactions of interest in fusion applications, the separation of short-ranged and long-ranged forces explicit in R-matrix theory [illegible] and angular momentum effects, like barrier penetration, to interact in a simple and natural way with nuclear effects, especially resonances. Also, since the R-matrix provides a particularly simple and unitary parameterization of multichannel [illegible], one has the prospect of [illegible] parameters to describe several [illegible] simultaneously, and of imposing a large amount of experimental information on the determination of the parameters, resulting in improved statistical reliability of predictions from the fit. In the following sections, we will describe applications of multichannel R-matrix theory to few-nucleon systems in the mass range A = 4-7 having charged-[illegible] of current interest in fusion applications. [illegible], however, with a brief, formal summary of R-matrix theory.

Formal Summary of R-Matrix Theory

Imagine a nuclear scattering process in which A [illegible], initially distributed between two bound particles, [illegible] distributed among [illegible] in general, be different from the initial [illegible]. Different [illegible] of the nucleons are [illegible] the arrangement channels of the system, and the surface [illegible] the [illegible] clusters is called the channel surface. [illegible] the short range of nuclear forces, the channel surface encloses only a relatively small region of configuration space for the nucleons. R-matrix theory relates the wavefunction in the large region outside the channel surface (which is most accessible to experiment) to that inside the channel surface [illegible]

[illegible]

$$H\Psi = E\Psi \quad [illegible]$$

[illegible]

$$[illegible]$$

[illegible]

$$= (H - E)^{-1} [illegible]$$

can be made hermitian in the internal region by the appropriate choice of [illegible], even though the hamiltonian H is not hermitian if [illegible] evolves to positive-energy channels at the surface.[8] A choice for [illegible] that accomplishes both purposes is

$$B = \sum_c [illegible] \left(\frac{\partial}{\partial r_c} r_c - b_c\right) [illegible], \quad (4)$$

with $[illegible] = \left(\frac{\hbar^2}{2m_c a_c}\right)^{1/2} \frac{\delta(r_c - a_c)}{a_c} Y_c(r_c)$, the "channel surface function", defined in terms of the channel spin-angle eigenfunction of total angular momentum and parity $Y_c(\hat{r}_c)$, and B_c the real, energy-independent boundary numbers specified at the channel surface $r_c = a_c$ which generate the R-matrix theory of Wigner and Eisenbud.[9]

Taking the projection of Eq. (2) on the channel surface, and inserting the forms (3) and (4), one obtains

$$(c'|\psi) = \sum (c'|G|c)(c|\frac{\partial}{\partial r_c} r_c - B_c|\psi) \quad . \tag{5}$$

Since ψ is known outside and on the channel surface (i.e., the "external" region) as a superposition of Coulomb spherical waves,

$$[illegible] = \sum_{c'} [illegible] \quad ,$$

the [illegible] in the external wavefunction can be expressed in terms of the elements of the R-matrix, [illegible]

[illegible]

where [illegible]

is the [illegible] derivative of the outgoing [illegible] Coulomb wavefunction evaluated on the surface. The unitarity of the collision matrix U follows from the hermiticity of the R-matrix. The point of expressing the collision matrix, from which the results of any scattering measurement – cross section, polarization, etc. – [illegible] in terms of the R-matrix [illegible] the properties of the internal [illegible]. The real and imaginary parts of [illegible] are usually called the "shift" and "penetrability" [illegible] the "hard sphere" phase shifts. [illegible]

[illegible] the familiar form for the R-matrix results. [illegible] eigenfunctions [illegible] satisfying

$$[illegible] \tag{8}$$

for eigenvalues E_λ form a complete orthogonal set in the internal region. Assuming the $|\lambda)$'s are normalized, we have the expansion

$$G = \sum_\lambda \frac{|\lambda)(\lambda|}{E_\lambda - E} \quad , \tag{9}$$

from which it follows immediately that

$$R_{c'c} = (c'|G|c) = \sum_\lambda \frac{\gamma_{\lambda c'}\gamma_{\lambda c}}{E_\lambda - E} \quad , \tag{10}$$

where $\gamma_{\lambda c} = (c|\lambda)$ is the "reduced width amplitude". The simple pole term of the R-matrix expansion (10), characterized by the parameters $\gamma_{\lambda c}$ and E_λ which depend on the channel radii a_c and boundary condition numbers B_c, can be identified with resonances of the compound A-nucleon system. However, not every pole term need be identified with a resonance in the conventional sense (i.e., one that shows a sufficiently narrow width Γ in the collision matrix to have a relatively long lifetime $\tau = h/\Gamma$). They can also be identified with shorter-lived "direct" processes, like single-particle scattering, stripping, etc., since the R-matrix formalism is not specialized to a particular reaction mechanism. Contributions from these latter processes are especially important in applications to few-nucleon systems, as those discussed in the following section.

Applications

We will describe multichannel R-matrix analyses of the [illegible] nucleon systems [illegible] contain some of the basic charged-particle fusion reactions, and which illustrate a wide range of R-matrix techniques being used at Los Alamos [illegible]. The general approach in these analyses has been to make use of all available data for all possible [illegible] reactions in each system, and to use the full multilevel, multichannel R-matrix expansion [illegible] approximated only by truncating the sum over levels [illegible]. For a given choice of channel radii a_c and boundary condition numbers B_c, the R-matrix parameters E_λ and $\gamma_{\lambda c}$ are adjusted by an automated fitting code, EDA,[11] to achieve a best fit in the least-squares sense to all the data included. The code also has the capability to treat the channel radii, as well as normalizations and energy shifts for the experimental data, as adjustable parameters.

Four Nucleons

We shall [illegible] reactions in the ^{4}He system, with [illegible] the R-matrix parameters [illegible] determined in such a way that [illegible] ^{3}He [illegible] system [illegible] ^{4}H system [illegible] scattering are also well represented. [illegible] the fact that the [illegible] Hamiltonian H, and thus the R-matrix [illegible] are [illegible] correct [illegible] symmetry of nuclear forces called charge independence, which is broken weakly by the internal Coulomb interaction. One then says that the R-matrix approximately conserves isospin (T), and in the case of the four-nucleon system, that the T = 1 part of the R-matrix which describes reactions in the ^{4}He system is essentially the same as that which describes p-^{3}He scattering, which, in turn, is essentially the same as that which describes n-T scattering. Accounting for the differences in the T = 1 R-matrix parameters due to internal Coulomb effects by simply shifting the E_λ's[7] appears to work quite well. The T = 1 parameters for this system were actually determined by fitting most of the available p-^{3}He scattering data below 20 MeV.[12] These parameters, energy-shifted to account for the decreased Coulomb repulsion energy in ^{4}He, were used in a larger analysis of reactions among p-T, n-^{3}He, and d-d where only the energy shift and parameters for the T = 0 part of the R-matrix were adjusted to fit the data. In addition, isospin conservation relates the widths in the p-T and n-^{3}He channels for both T = 0 and T = 1 levels to reduce further the number of parameters.

A summary of the data included for each reaction in the ^{4}He system analysis is given in Table I. The types of data to which the table refers generally

include cross sections (both differential and integrated) and polarizations for various spin orientations of the incoming and outgoing particles. The fits are, on the whole, good representations of the experimental measurements for all six reactions.

Table I. ^{4}He System Analysis

CHANNELS INCLUDED:	p-T n-^{3}He d-d		
Ref. [1]	Energy Range (MeV)	No. Observable Types	No. Data Points
T(p,p)	E_p=0-2.1	2	1317
T(p,n) ^{3}He-ints.	E_p=0-2.1	5	723
^{3}He(n,n) ^{3}He	E_n=0-2.1	2	117
T(d,p)	E_d=0-2.1	6	693
D(d,n) ^{3}He	E_d=0-2.1	6	543
D(d,d)	E_d=0-2.0	2	705
	TOTALS:	23	4108

[illegible], however, a noticeable exception to the overall quality of the fit is the low-energy cross section data for the two branches of the d + d reaction, which are the most relevant to the fusion system of current fusion interest. The character of the experimental measurements[13] show large differences in the D(d,n) ^{3}He and D(d,p)T cross sections in the few-hundred keV range. The D(d,n) differential cross section has a higher zero-to-ninety-degree asymmetry than does the D(d,p) differential cross section, and the integrated cross section for the neutron branch lies 15-2[illegible]% higher than that for the proton branch. These differences are quite unexpected at first glance, because they occur for mirror reactions which we would expect to be more similar on the basis of charge symmetry. Even taking into account external charge differences in the exit-channel (n-^{3}He and p-T) penetrabilities, etc., would appear to give the opposite effect to that observed - ie, the enhancement of the proton branch. However, we noticed a compensating enhancement of the neutron branch in the p-wave states coming from isospin mixing in the external Coulomb field, although it was not sufficient to explain the experimentally observed differences.

Recently, following the suggestion of Sergeyev[14] that additional isospin mixing from the internal Coulomb interactions may reproduce the observed differences, we have allowed non-zero T = 1 widths in the ^{3}P states of the d-d channel (these widths are zero in the strict isospin-conservation limit). Indeed, the experimental differences are largely reproduced with mixing widths only 2% of the single-particle value which characterizes the d-d widths in the ^{3}P, T = 0 levels. This is entirely consistent with the magnitude of the matrix element one might expect from internal Coulomb mixing, indicating that perhaps anomalous differences even as large as those observed in the d + d reaction cross sections may be explained entirely by Coulomb effects.

The calculations are compared to low-energy measurements of the D(d,n) and D(d,p) cross sections in Figs. 1 and 2. Figure 1 shows the isospin-mixed D(d,n) and D(d,p) integrated cross section calculations compared with various measurements at energies below 500 keV. Figure 2 shows the effect of

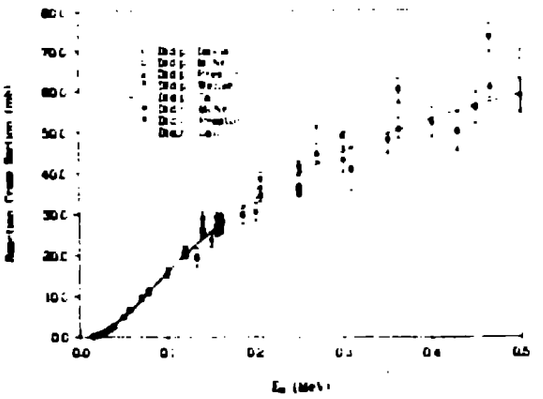

Fig. 1. R-matrix fits (solid curves) to various measurements of the D(d,n)^{3}He (upper points) and D(d,p)T (lower points) cross sections at energies below 500 keV.

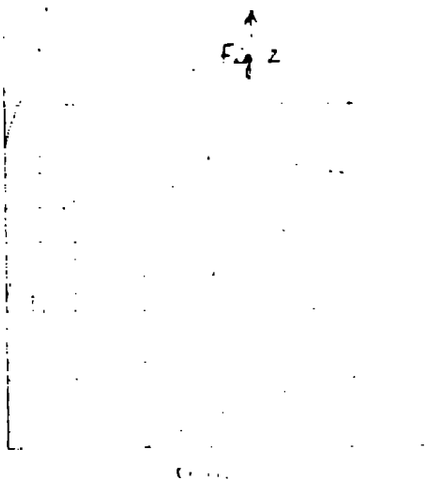

Fig. 2

Fig. 2. Ratios of the integrated cross sections, $\frac{\sigma_n}{\sigma_p}$, and of the Asymmetries, $\frac{\sigma_n(0)}{\sigma_n(90)} / \frac{\sigma_p(0)}{\sigma_p(90)}$, for the two branches of the d + d reaction. The points are measurements of Theus et al; the solid and dashed curves are R-matrix calculations with and without internal isospin mixing, respectively.

allowing internal isospin mixing in the calculations on the ratio of the integrated cross sections, and on the ratio of the differential cross section asymmetries for the two reactions. The large values of these ratios observed experimentally in the few-hundred keV region are clearly much better reproduced by including internal isospin mixing in the calculations.

The calculations including internal isospin mixing also show improved agreement with differences in the outgoing neutron and proton polarizations measured at low energies. At higher energies, where differences have been seen to persist in measurements of analyzing powers for the two reactions both with polarized deuterons,[23,24] the situation is not so clear. Some of the analyzing-power differences are improved by the mixing, while others remain unaccounted for. We plan to explore the effect of allowing internal isospin mixing in higher partial waves on these analyzing powers. In addition, we need to investigate a related consequence of internal isospin mixing that has been neglected thus far: the perturbation of the pure isospin relation between p-T and n-^{3}He widths in both the T = 0 and T = 1 levels. However, the results of the analysis at this stage show promise for being able to account sucessfully for data **from all the four-nucleon reactions with a single, Coulomb-corrected, charge-independent set of R-matrix** parameters.

Five Nucleons

The discussion here will concern mainly reactions in the ^{5}He system, which contains the most prominent of all low-energy fusion processes, T(d,n)^{4}He. A summary of the channels and data included in the ^{5}He analysis is given in Table II. It can be seen that an especially large variety of data types is available for the T(d,n) reaction, including cross sections, measurements for beam and target polarized separately (analyzing powers) and simultaneously (spin correlations), and measurements of outgoing neutron polarizations for both unpolarized and polarized (polarization transfer) configurations of beam and target.

Table II. ^{5}He System Analysis

CHANNELS INCLUDED: d-t
n-^{4}He
n-^{4}He*

Reaction	Energy Range (MeV)	No. Observable Types	No. Data Points
T(d,d)T	E_d=0-8	6	752
T(d,n)^{4}He	E_d=0-8	13	852
T(d,n)^{4}He*	E_d=4.8-8	1	11
^{4}He(n,n)^{4}He	E_n=0-28	2	799
	TOTALS:	22	2414

The fits to a small sample of the 2400 data points are shown for the reactions T(d,d)T, T(d,n)^{4}He, and ^{4}He(n,n)^{4}He in Figs. 3-5. Figure 3 shows cross section and polarization angular distributions for T(d,d)T in the range E_d = 1.2 to 8 MeV. Figure 4 shows fits to a selection of the T(d,n)^{4}He data at energies between 1 and 7 MeV; cross sections and polarizations for ^{4}He(n,n)^{4}He at neutron energies between 1.6 and 24 MeV are shown in Fig. 5. These are representative of the fits to all the data included in the analysis, which are generally quite good.

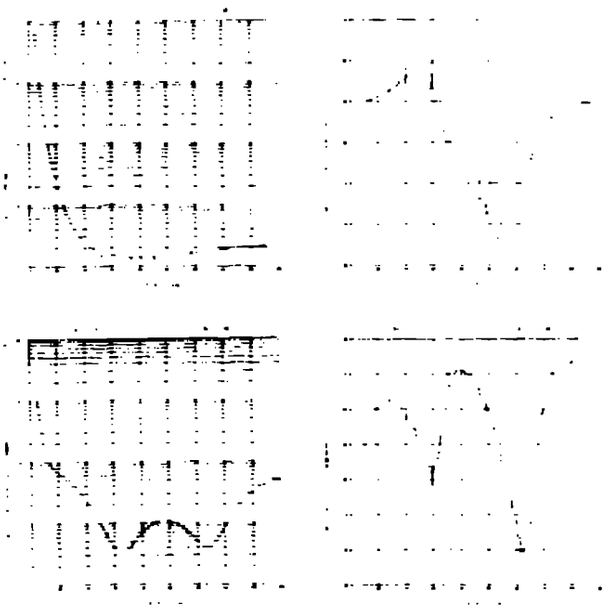

Fig. 3. Fits to T(d,d)T cross sections and analyzing powers at energies between 1.2 and 8 MeV.

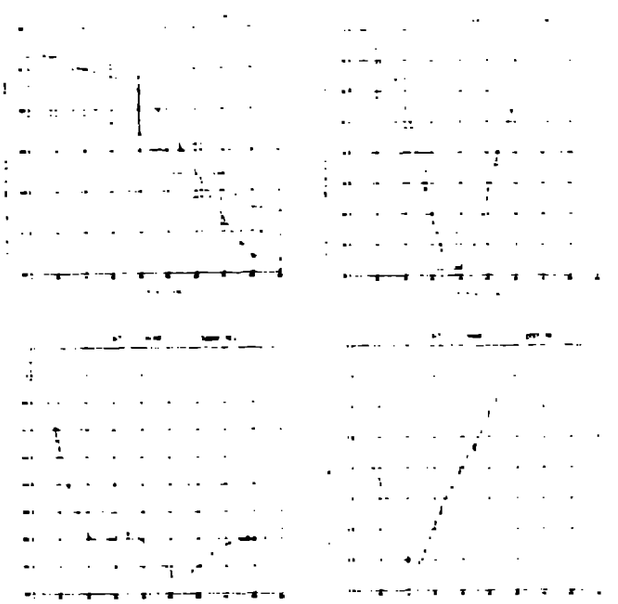

Fits to T(d,n)^{4}He cross sections and polarization at energies between 1 and 7 MeV.

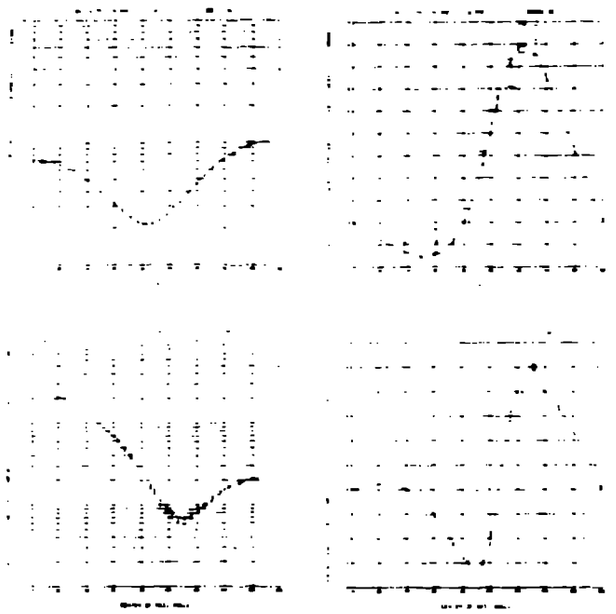

Fig. 5. Fits to ^{4}He(n,n)^{4}He cross sections and polarizations at energies between 0.9 and 24 MeV.

The calculated and measured observables for this system, particularly the polarizations, undergo marked changes in angular shape as a function of energy over the range of the analysis (E_x < 22 MeV), due in part to the presence of ten "resonances" at excitation energies E_x < 25 MeV in ^{5}He. Only two of these produce visible structure in the integrated T(d,n) reaction cross section shown in Fig. 6. One is the famous 110-keV resonance responsible for the large low-energy cross section which makes the T(d,n) reaction such an attractive fusion energy process, and the other is a small "bump" at E_d ~ 4.5 MeV.

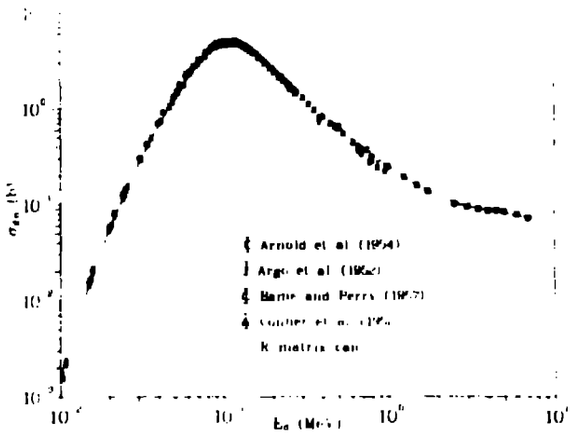

Fig. 6. R-matrix calculation (solid curve) compared to various measurements of the T(d,n)^{4}He integrated cross section at energies below 8 MeV.

The effect of the 110-keV s-wave resonance on the T(d,n) cross section persists down to very low deuteron energies. This can be seen in an expanded plot of the low-energy cross sections shown in Fig. 7, in which the inverse-energy and Gamow-penetrability dependence have been removed. What remains, the so-called "astrophysical S-function", would plot as a horizontal straight line if the assumptions implied by the usual Gamow extrapolation of the low-energy cross sections were valid. In fact, the dashed line labeled "Gamow extrapolation" corresponds to the cross section values reported by Arnold et al.[17] in place of their own experimental measurements[18] ( ) at energies below 20 keV. The R-matrix calculation clearly does not follow the Gamow dependence at low energies due to the resonance, and tends to confirm the behavior of the original measurements.[18]

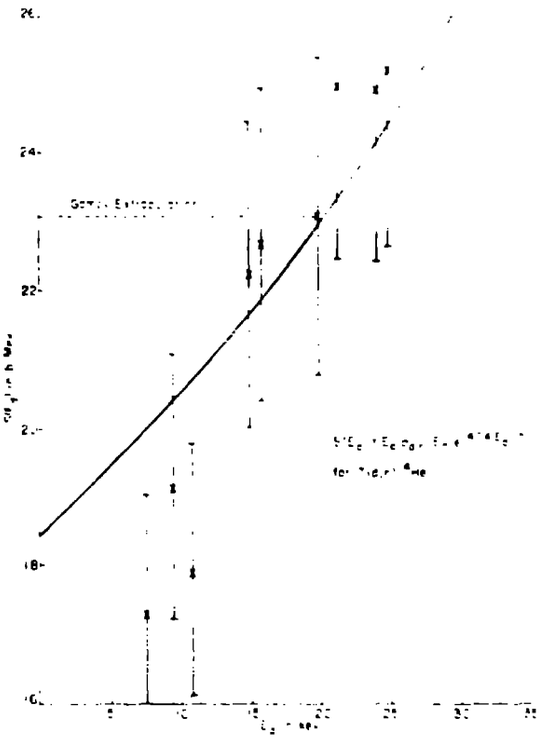

Fig. 7. Astrophysical S-function for T(d,n)^{4}He as a function of laboratory energy. The solid curve is the R-matrix calculation, and the dashed line is the Gamow extrapolation reported by Arnold et al.[17] in place of their measured points[18] ( ) at energies below 20 keV.

We are also doing a similar analysis of reactions in the ^{5}Li (d-^{3}He, p-^{4}He) system which uses an even more extensive data base. The calculated ^{3}He(d,p)^{4}He integrated cross section we obtain peaks at a value nearly in the middle of the broad range of measured values that have been obtained at the peak - from 700 to 900 mb. Neither of the five-nucleon analyses is yet final, since new measurements have been added recently in both cases which appear to conflict with some of the data previously being analyzed, but the essential features of the calculated reaction cross sections discussed here have not changed.

Six Nucleons: ^{6}He System

Our study of reaction in ^{6}He system is motivated by large uncertainties in the T(t,2n)^{4}He cross section

at low energies, corresponding to large discrepancies among the measurements. As can be seen in Table III, very few measurements are available for reactions in this system, making this analysis an example of one of the simplest we have yet done.

Table III. ^{6}He System Analysis

CHANNELS INCLUDED: t-T
n-^{5}He (2n-^{4}He)

Reaction	Energy Range (MeV)	No. Observable Types	No. Data Points
T(t,t)T	E_t=0-2	1	27
T(t,2n)^{4}He	E_t=0-2	1	71
	TOTALS:	2	98

The fits to most of the few available t-t differential elastic scattering cross section measurements are shown in Fig. 8 at triton energies between 1.6 and 2 MeV. Although these fits are quite good, it is doubtful whether they constrain very much the fit to the T(t,2n) reaction cross sections shown in Fig. 9, particularly at low energies. Nevertheless, the R-matrix calculation shows a definite preference for the relatively recent measurements of Serov et al.[19] in the low-energy region. This remains the case even when the Serov data are removed from the fit, indicating that the low-energy behavior of the calculated cross section is actually being determined by consistency with the data at energies above 100 keV, where the measurements are in much better mutual agreement. Of course, the low-energy extrapolation of the cross section is to some extent a function of the extremely simple parameterization of the R-matrix necessitated by lack of data, but the agreement with the Serov data is an indication that this parameterization may be adequate at energies below 2 MeV. In particular, we take into account only contributions from the ^{6}He ground state, and from a level which is responsible for the slight bump in the t+t reaction cross section at energies close to 2 MeV.

Large differences between our calculated curve and some of the earlier measurements at energies below 100 keV (see Fig. 9) result in significant differences between Maxwellian reaction rates calculated from the R-matrix cross sections and those based on the earlier data. Our reaction rates become a factor of two or more lower than those of Greene[21] and of Duane[22] at temperatures below kT = 10 keV.

Seven Nucleons

Although the analysis discussed here is a charge-symmetic R-matrix analysis of all the 7-nucleon reactions, including those in both the ^{7}Li and ^{7}Be systems, we shall mention only the ^{7}Be reactions. This is because similar analyses of reactions in the ^{7}Li system have been discussed elsewhere[5,6,23] in connection with neutron standards applications, and because the ^{7}Be system contains charged-particle reactions of great interest in advanced fusion concepts.[2]

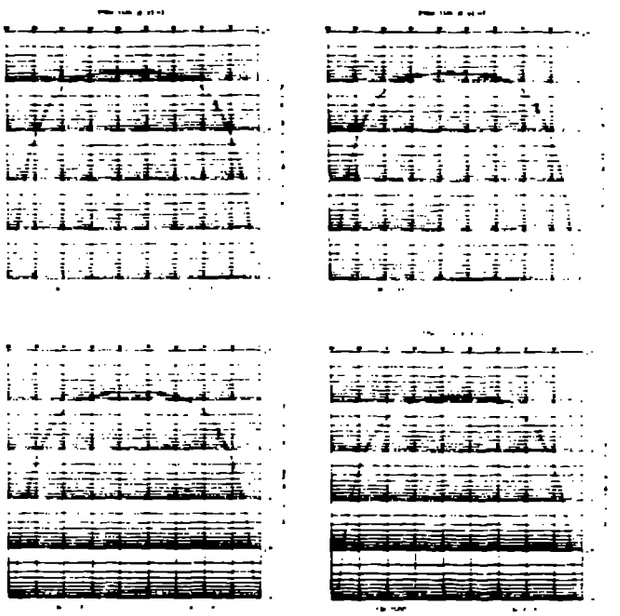

Fig. 8. Fits to T(t,t)T differential cross sections at energies between 1.6 and 2 MeV.

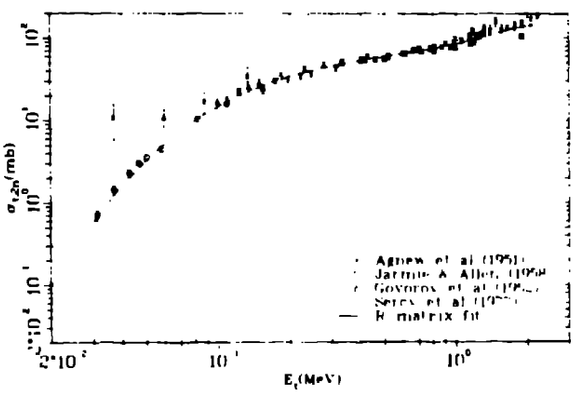

Fig. 9. R-matrix calculation (solid curve) compared with various measurements of the T(t,2n)^{4}He integrated cross section at energies below 2 MeV.

A summary of the data included for the 7-nucleon reactions is given in Table IV. Cross section and polarization measurements are available for the four reactions possible among p-^{6}Li and ^{3}He-^{4}He (^{7}Be system). The fits to some of these are shown for the three independent reactions ^{6}Li(p,p)^{6}Li, ^{6}Li(p,^{3}He)^{4}He, and ^{4}He(^{3}He,^{3}He)^{4}He in Figs. 10-12.

The problem in the ^{6}Li(p,^{3}He)^{4}He reaction, which is of greatest current interest in the ^{7}Be system, has been that the few existing differential cross section measurements have been relative, and the absolute determinations of the integrated cross section have differed by as much as 50%. In the 7-nucleon analysis we described at the Harwell conference[7] as an example of our charge-independent approach, the

Table IV. Seven-Nucleon Analysis

CHANNELS INCLUDED: $p\text{-}^{6}Li$ $n\text{-}^{6}Li$ $^{3}He\text{-}^{4}He$ $t\text{-}^{4}He$

Reaction	Energy Range (MeV)	No. Observ-able Types	No. Data Points
$^{6}Li(p,p)^{6}Li$	E_p=0-2.5	1	187
$^{6}Li(p,^{3}He)^{4}He$-inv.	E_p=0-2.5	3	559
$^{4}He(^{3}He,^{3}He)^{4}He$	$E_{^{3}He}$=0-11	2	1467
$^{6}Li(n,n)^{6}Li$	E_n=0-1.7	3	330
$^{6}Li,(n,t)^{4}He$	E_n=0-1.7	2	468
$^{4}He,(t,t)^{4}He$	E_t=0-11	2	1355
	TOTALS:	13	4386

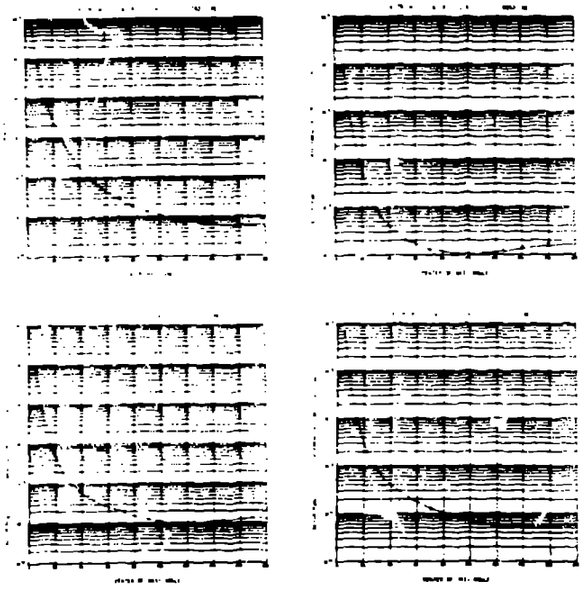

Fig. 10. Fits to $^{6}Li(p,p)^{6}Li$ cross sections at energies below 2.5 MeV.

experimental cross-section data included for the $^{6}Li(p,^{3}He)$ reaction required extensive renormalization in almost every case. We have therefore been uncertain about the reliability of the scale of our calculated cross sections, which presumably was determined by data for other reactions in the analysis.

Recently, new absolute measurements of $^{6}Li(p,^{3}He)^{4}He$ differential cross sections at proton energies between 0.14 and 3 MeV have been made by Elwyn et al.[22] at Argonne National Laboratory. A comparison of their integrated cross sections with our predictions[7] is shown in Fig. 13. It can be seen that the agreement of the calculations with the new measurements is excellent, both in shape and magnitude.

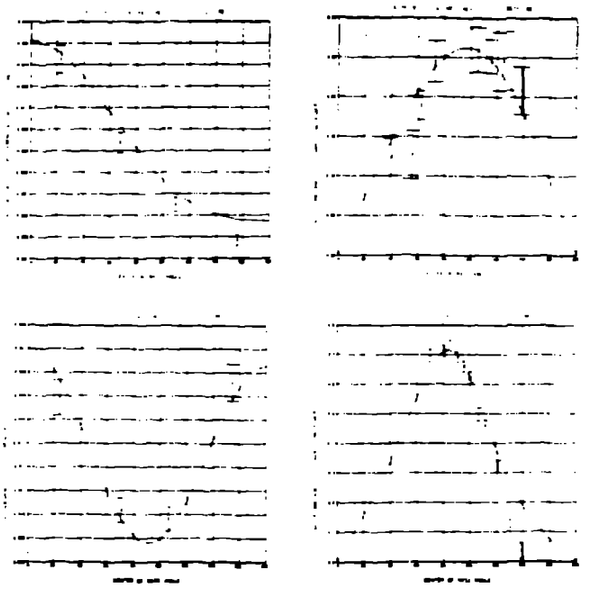

Fig. 11. Fits to $^{6}Li(p,^{3}He)^{4}He$ cross sections and polarizations at energies below 2.5 MeV.

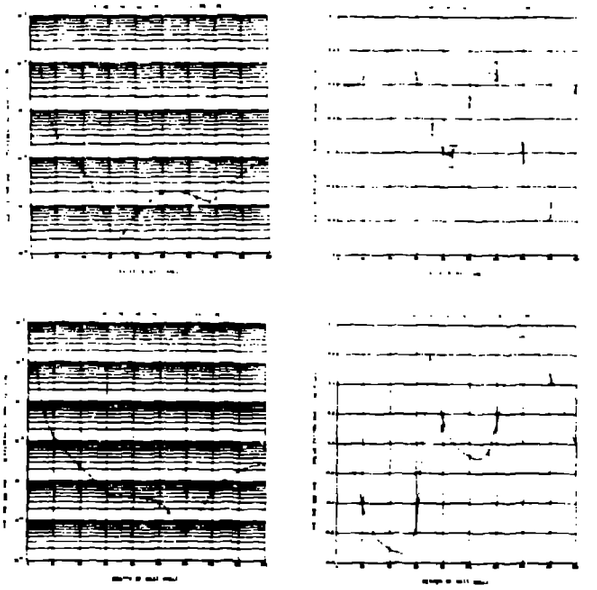

Fig. 12. Fits to $^{4}He(^{3}He,^{3}He)^{4}He$ cross sections and polarizations at energies below 10 MeV.

The agreement of the calculated angular distributions with the new data[22] is generally poorer, especially at energies above 2 MeV, indicating that somewhat different interferences among the partial-wave amplitudes are required (possibly even those involving $p\text{-}^{6}Li$ d-waves, which have been neglected thus far in the calculations) which do not affect the integrated cross sections

This comparison indicates that the other 7-nucleon data in the analysis, through unitary and charge-

conjugate relationships, correctly determine the scale of the $^{6}Li(p,^{3}He)$ reaction cross section, much as other ^{7}Li data had constrained values of the $^{6}Li(n,t)$ cross section in the analysis[23] used for the ENDF/B-V ^{6}Li evaluation at low energies.

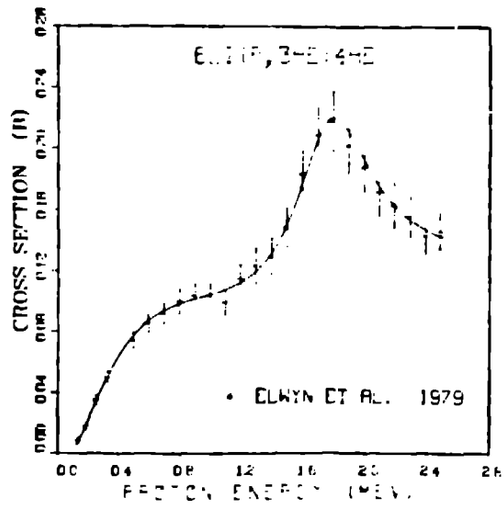

Fig. 13. Predictions from the charge-symmetric 7-nucleon analysis[7] compared with recent measurements of Elqyn et al.[22] for the $^{6}Li(p,^{3}He)^{4}He$ integrated cross section.

Conclusions

As the examples described in the previous section suggest, a great deal of information is available from these multireaction R-matrix analyses, having been determined in most cases by a large and varied collection of experimental input. Clearly, the R-matrix parameters provide detailed information about the spectroscopy of light systems, and even information about the macroscopic properties of nuclear forces. Of more direct concern to the subject of this conference, however, are the smooth (as functions of both energy and angle) charged-particle cross sections which result from them.

The dominance of Coulomb effects in charged-particle cross sections at low energies is modified by nuclear resonances in many cases of interest in fusion applications. This is most apparent for the T(d,n) reaction, but is true to some degree for all the reactions discussed. R-matrix theory provides a framework for fitting and extrapolating these cross sections in which both the long-range effects, like penetration of the Coulomb-angular momentum barrier, and the short-range (nuclear) effects arise in a simple and physically meaningful way. Moreover, the interaction of these effects in the theory leads in general to a different energy dependence for the low-energy cross sections than that obtained from the representations of fusion cross sections commonly used.[24] There are indications from the T(d,n) and T(t,2n) examples that the R-matrix dependence is more nearly correct, but a firm conclusion requires more and better-quality measurements in the low-energy region, such as those forthcoming from the fusion cross-section measurement program at Los Alamos.[3]

At higher energies, the reactions appear to be dominated by broad, overlapping structures, few of which appear as definite bumps in the integrated cross sections. These structures can be associated with definite R-matrix levels, however, with the help of angular distribution measurements, particularly those for polarization observables. Attempting to use all the available experimental data in these analyses also has obvious statistical advantages, especially in cases where direct measurements of the cross sections are conflicting or incomplete. In these cases, the other data included, even for different reactions, can help dictate more correct values for cross sections, as illustrated by the $p+^{6}Li$ example.

We feel that such R-matrix analyses, making maximal use of the available experimental data while imposing some minimal information about nuclear forces, constitute the best technique currently at hand for evaluating light-element cross sections. One obtains from these analyses unified cross-section sets, in which the elastic scattering and reaction cross section for a given system are calculated from the same R-matrix parameters. We therefore suggest that compilers of evaluated charged-particle cross sections make use of these calculations, where available, rather than rely on methods having less physical content and experimental input.

Acknowledgments

K. Witte, who developed and maintains the EDA code, has been our collaborator on several of these analyses. Likewise, S. D. Baker and E. K. Biegert collaborated with us on analyses of the 7-nucleon reactions.

References

1. C. R. Head, "Nuclear Data Requirements of the Magnetic Fusion Power Program of the United States of America," presented at IAEA Advisory Group Meeting on Nuclear Data for Fusion Reactor Technology, Vienna, Austria (1978).

2. R. W. Conn, Bull. Am. Phys. Soc. 24, 866 (1979).

3. N. Jarmie, Bull. Am. Phys. Soc. 24, 865 (1979).

4. D. C. Dodder et al., "Models Based on Multichannel R-Matrix Theory," JAERI-M 5984, p. 1 (1975).

5. G. M. Hale, "R-Matrix Analysis of the Light Element Standards," NBS Special Publication 425, p. 302 (1975).

6. G. M. Hale, "R-Matrix Methods for Light Systems," IAEA-90, Vol. II, p. 1 (1976).

7. D. C. Dodder and G. M. Hale, "Applications of Approximate Isospin Conservation in R-Matrix Analyses," in Neutron Physics and Nuclear Data (Harwell), p. 490 (1978).

8. A. M. Lane and D. Robson, Phys. Rev. 151, 774 (1966).

9. E. P. Wigner and L. Eisenbud, Phys. Rev. 72, 29 (1947).

10. A. M. Lane and R. G. Thomas, Rev. Mod. Phys. 30, 257 (1958).

11. D. C. Dodder, K. Witte, and G. M. Hale, "EDA, an Energy Dependent Analysis Code for Nuclear Reactions," (unpublished).

conjugate relationships correctly determine the scale of the $^{6}Li(p,^{3}He)$ reaction cross section, much as other ^{7}Li data had constrained values of the $^{6}Li(n,t)$ cross section in the analysis[23] used for the ENDF/B-V ^{6}Li evaluation at low energies.

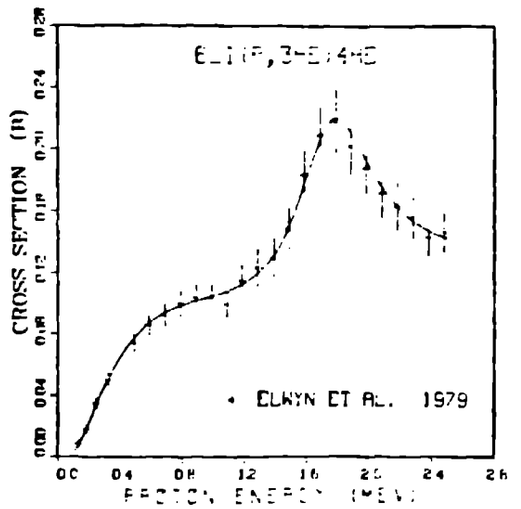

Fig. 13. Predictions from the charge-symmetric 7-nucleon analysis[7] compared with recent measurements of Elqyn et al.[22] for the $^{6}Li(p,^{3}He)^{4}He$ integrated cross section.

Conclusions

As the examples described in the previous section suggest, a great deal of information is available from these multireaction R-matrix analyses, having been determined in most cases by a large and varied collection of experimental input. Clearly, the R-matrix parameters provide detailed information about the spectroscopy of light systems, and even information about the macroscopic properties of nuclear forces. Of more direct concern to the subject of this conference, however, are the smooth (as functions of both energy and angle) charged-particle cross sections which result from them.

The dominance of Coulomb effects in charged-particle cross sections at low energies is modified by nuclear resonances in many cases of interest in fusion applications. This is most apparent for the T(d,n) reaction, but is true to some degree for all the reactions discussed. R-matrix theory provides a framework for fitting and extrapolating these cross sections in which both the long-range effects, like penetration of the Coulomb-angular momentum barrier, and the short-range (nuclear) effects arise in a simple and physically meaningful way. Moreover, the interaction of these effects in the theory leads in general to a different energy dependence for the low-energy cross sections than that obtained from the representations of fusion cross sections commonly used.[24] There are indications from the T(d,n) and T(t,2n) examples that the R-matrix dependence is more nearly correct, but a firm conclusion requires more and better-quality measurements in the low-energy region, such as those forthcoming from the fusion cross-section measurement program at Los Alamos.[3]

At higher energies, the reactions appear to be dominated by broad, overlapping structures, few of which appear as definite bumps in the integrated cross sections. These structures can be associated with definite R-matrix levels, however, with the help of angular distribution measurements, particularly those for polarization observables. Attempting to use all the available experimental data in these analyses also has obvious statistical advantages, especially in cases where direct measurements of the cross sections are conflicting or incomplete. In these cases, the other data included, even for different reactions, can help dictate more correct values for cross sections, as illustrated by the $p+^{6}Li$ example.

We feel that such R-matrix analyses, making maximal use of the available experimental data while imposing some minimal information about nuclear forces, constitute the best technique currently at hand for evaluating light-element cross sections. One obtains from these analyses unified cross-section sets, in which the elastic scattering and reaction cross section for a given system are calculated from the same R-matrix parameters. We therefore suggest that compilers of evaluated charged-particle cross sections make use of these calculations, where available, rather than rely on methods having less physical content and experimental input.

Acknowledgments

K. Witte, who developed and maintains the EDA code, has been our collaborator on several of these analyses. Likewise, S. D. Baker and E. K. Biegert collaborated with us on analyses of the 7-nucleon reactions.

References

1. C. R. Head, "Nuclear Data Requirements of the Magnetic Fusion Power Program of the United States of America," presented at IAEA Advisory Group Meeting on Nuclear Data for Fusion Reactor Technology, Vienna, Austria (1978).

2. R. W. Conn, Bull. Am. Phys. Soc. 24, 868 (1979).

3. N. Jarmie, Bull. Am. Phys. Soc. 24, 868 (1979).

4. D. C. Dodder et al., "Models Based on Multichannel R-Matrix Theory," JAERI-M 5984, p. 1 (1975).

5. G. M. Hale, "R-Matrix Analysis of the Light Element Standards," NBS Special Publication 425, p. 302 (1975).

6. G. M. Hale, "R-Matrix Methods for Light Systems," IAEA-90, Vol. II, p. 1 (1976).

7. D. C. Dodder and G. M. Hale, "Applications of Approximate Isospin Conservation in R-Matrix Analyses," in Neutron Physics and Nuclear Data (Harwell), p. 490 (1978).

8. A. M. Lane and D. Robson, Phys. Rev. 151, 774 (1966).

9. E. P. Wigner and L. Eisenbud, Phys. Rev. 72, 29 (1947).

10. A. M. Lane and R. G. Thomas, Rev. Mod. Phys. 30, 257 (1958).

11. D. C. Dodder, K. Witte, and G. M. Hale, "EDA, an Energy Dependent Analysis Code for Nuclear Reactions," (unpublished).

12. G. M. Hale, J. Devaney, D. C. Dodder, and K. Witte, Bull. Am. Phys. Soc. 19, 506 (1974).

13. See, for instance, R. B. Theus, W. I. McGary, and I. A. Beach, Nucl. Phys. 80, 279 (1966).

14. V. A. Serpeyev, Phys. Lett. 38B, 246 (1972).

15. V. Kulik et al., "Investigation of Charge Symmetry Violation in the Mirror Reactions ^{2}H(d,γ)^{3}H and ^{2}H(d,γ)^{3}He," submitted to Nucl. Phys. (1979).

16. I. R. Donnelly, Ohio State University, personal communication (1979).

17. W. R. Arnold et al., Phys. Rev. 93, 483 (1954).

18. W. R. Arnold et al., "Absolute Cross Section for the Reaction T(d,n)He^{4} from 10 to 120 keV," LA-1574 (1953).

19. V. I. Serov, S. N. Abramovich, and L. A. Morkin, At. Ener. 44, 59 (1977).

20. S. L. Greene, "Maxwell Averaged Cross Sections for Some Thermonuclear Reactions on Light Isotopes," UCRL-70522 (1967).

21. B. H. Duane, "Fusion Cross Section Theory," BNWL-1685, p. 75 (1972).

22. A. J. Elwyn et al., "Cross Sections for the ^{6}Li(n,^{3}He)^{4}He Reaction at Energies Between 0.1 and 1.7 MeV," submitted to Phys. Rev. C (1979).

23. G. M. Hale, "R-Matrix Analysis of the ^{7}Li System," NBS Special Publication 425, p. 90 (1977).

24. In these representations, resonance effects are not explicit in the S-functions. The simplest example is the Gamow extrapolation of cross sections. Other examples are Refs. 21, Ref. 23, and A. Lane, Ann. Phys. (N.Y.) 63, 171 (1971).